

Magnetization Jump in the Magnetization Process of the spin-1/2 Heisenberg Antiferromagnet on a Distorted Square-Kagome Lattice

Hiroki Nakano¹ *, Yasumasa Hasegawa¹ †, and Tôru Sakai^{1,2} ‡

¹Graduate School of Material Science, University of Hyogo, Kamigori, Hyogo 678-1297, Japan

²Japan Atomic Energy Agency, SPring-8, Sayo, Hyogo 679-5148, Japan

(Received December 21, 2021)

We study the magnetization process of the spin-1/2 Heisenberg antiferromagnet on a distorted square-kagome lattice by the numerical-diagonalization method. The magnetization jump at one-third of the height of the saturation is examined in detail; we find that the jump becomes larger when a small distortion is switched on and that it is accompanied by an abrupt change in lines along microscopic spin directions. Our finite-size results successfully confirm that the magnetization jump in a spin-isotropic system is a macroscopic jump that survives in the thermodynamic limit and that the changes in spin directions are common to a spin-flop phenomenon observed in spin-anisotropic systems.

1. Introduction

Frustration has attracted much attention in condensed matter physics because it plays an important role as an origin of nontrivial behaviors in various systems. Particularly, such nontrivial behaviors are often observed in magnetic materials. One of them is the magnetization plateau. A magnetization plateau is the appearance of a region of a magnetic field in a magnetization process where the magnetization does not increase even with an increase in the magnetic field. This phenomenon is in contrast to a normal case, in which a magnetization process shows a smooth and significant increase in magnetization with an increase in magnetic field. Such a plateau originates from the existence of an energy gap between levels in magnetic fields owing to the formation of an energetically stable quantum spin state, for example, the spin-1 alternating spin chain¹ and two-dimensional orthogonal dimer system.²

Another nontrivial behavior is the magnetization jump. During a jump in the magnetization process, the increase in magnetization is discontinuous, in contrast to the fact that a magnetization plateau corresponds to a discontinuity with respect to the magnetic field. As an origin of such magnetization jumps, a spin-flop phenomenon is well known.³ The phenomenon is the occurrence of an abrupt change in lines along microscopic spin directions while the states change owing to the increase in magnetic field. It is widely known that the phenomenon occurs when the system includes anisotropy in spin space.^{4,5} Under these circumstances, there was a report of an interesting system that shows a magnetization jump even when the system has no anisotropy in spin space; the system is the spin-1/2 Heisenberg antiferromagnet on the square-kagome lattice.⁶

This lattice is originally introduced in the study of the relationship between the spin model on this lattice

and the eight-vertex model;⁷ numerical-diagonalization studies of the quantum system on this lattice were carried out^{8,9} although the above jump was not recognized within these studies. The lattice shares several characteristics with the kagome lattice; for example, the coordination number $z = 4$ from a vertex of each lattice is the same. The corner sharing of neighboring local triangles is also the same. We hereafter call the structure of each unit cell a *shuriken* from its shape. The most important difference between the kagome and square-kagome lattices is whether or not all the vertices are equivalent with respect to the polygons that surround a focused vertex. In the square-kagome lattice, vertices are divided into two groups: one that is a vertex of the small square inside the local structure of a *shuriken* and one that is not (see Fig. 1). Let us call a vertex site in the former (latter) group the α (β) site hereafter. This difference induces nontrivial different behaviors between the magnetization processes of these two systems. In the kagome-lattice antiferromagnet, there is a region similar to a magnetization plateau at one-third height of the saturation. Just outside of this height, the change in the magnetization is continuous but the magnetization process shows a nontrivial critical behavior, which is certainly different from a magnetization plateau of the well-known type in a two-dimensional system.¹⁰⁻¹² Although there appears a magnetization plateau at the same height in the square-kagome-lattice antiferromagnet, the plateau was found to be accompanied by a discontinuous change in the magnetization at the edge of the higher-field side in the magnetization processes of finite-size clusters. The discontinuity strongly suggests a magnetization jump. The local magnetization also shows its discontinuity, which suggests that a behavior similar to a spin-flop phenomenon happens. A common behavior in finite-size clusters is observed in other cases: the Cairo-pentagon lattice,^{13,14} the distorted kagome lattice,^{12,15} and the *shuriken*-bonded honeycomb lattice.¹⁵

However, to confirm that this discontinuous behavior of finite-size clusters in the square-kagome-lattice

*E-mail: hnakano@sci.u-hyogo.ac.jp

†E-mail: hasegawa@sci.u-hyogo.ac.jp

‡E-mail: sakai@spring8.or.jp

antiferromagnet corresponds to a true magnetization jump owing to a spin-flop phenomenon, the following two viewpoints should be clarified. One is whether or not the jump certainly survives in the thermodynamic limit. In a normal magnetization process without any anomalies, the increase in magnetization of a finite-size cluster must be $\delta M = 1$; in the square-kagome-lattice antiferromagnet, a discontinuity of $\delta M = 2$ was found. Note here that a discontinuity of $\delta M = 2$ can appear in the spin-nematic state.^{16,17} Since the spin-nematic state is the two-spin magnon state, the discontinuity of the spin-nematic state is not a macroscopic behavior. To exclude the possibility that a discontinuity of $\delta M = 2$ in the square-kagome-lattice antiferromagnet indicates the spin-nematic state, it is sufficient to observe a discontinuity of $\delta M \geq 3$. The other point is how the transverse spin component behaves. The local magnetization examined in Ref. 6 provides information on a component along the external field, namely, the z -axis. If the transverse spin component between both sides at the observed jump shows a significant difference, the relationship between the magnetization jump and the spin-flop phenomenon is established. Under these circumstances, the purpose of this study is to clarify these two unresolved issues in the square-kagome-lattice antiferromagnet by taking distortion into account additionally to the undistorted square-kagome-lattice case.

Candidate square-kagome-lattice antiferromagnet materials have not been reported so far to the best of our knowledge. On the other hand, the discoveries of candidate kagome-lattice antiferromagnet materials such as herbertsmithite,^{18,19} volborthite,^{20–22} and vesignieite,^{23,24} have accelerated experimental studies as well as theoretical ones,^{25–45} leading to a deeper understanding of the physics of the kagome-lattice antiferromagnet. From these studies, it is gradually clarified that the materials have significant deviations from the ideal situation of the kagome-lattice Heisenberg antiferromagnet. In volborthite, for example, magnetic interactions deviate from the uniform situation in the kagome lattice because of the orbital directions despite the fact that atomic positions are located at the vertices of the kagome lattice. To understand the candidate materials well, therefore, effects due to the deviation from the ideal situation are worth studying, which is a background of this study.

This paper is organized as follows. In the next section, the model that we study here is introduced. The method and analysis procedure are also explained. The third section is devoted to the presentation and discussion of our results. We first discuss the change in local magnetizations of the state at one-third of the height of the saturation. The discussion will clarify which phase the undistorted square-kagome-lattice case is located in. After that, the magnetization process of larger clusters is presented. The spin-spin correlations are also examined. In the final section, we present our conclusion.

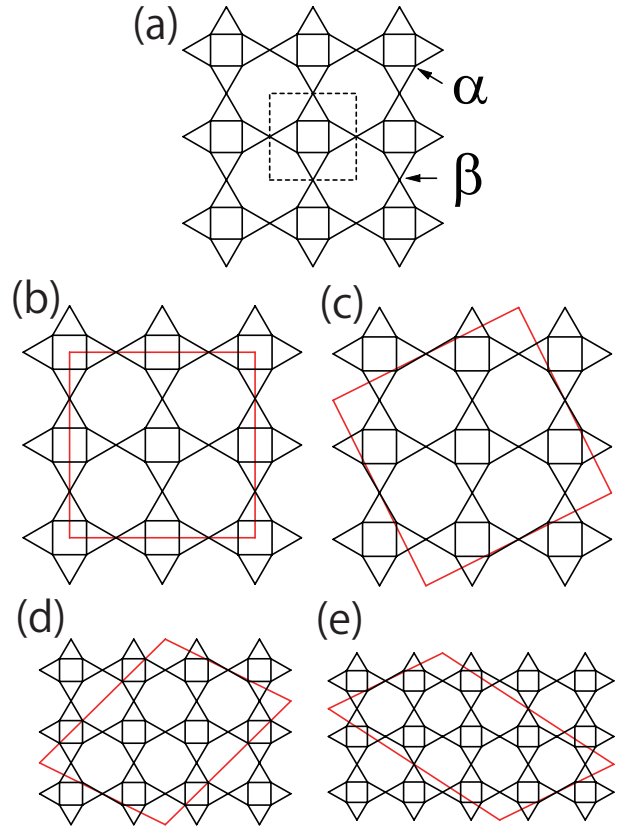


Fig. 1. (Color) Structure of the square-kagome lattice. In panel (a), α and β sites are illustrated; the broken-line square represents a unit cell of this lattice. The shapes of finite-size clusters studied in this work are shown for (b) $N_s = 24$, (c) $N_s = 30$, (d) $N_s = 36$, and (e) $N_s = 42$.

2. Model Hamiltonians and Method

The Hamiltonian that we study in this work is given by $\mathcal{H} = \mathcal{H}_0 + \mathcal{H}_{\text{Zeeman}}$, where

$$\mathcal{H}_0 = \sum_{\langle i,j \rangle, i \in \alpha, j \in \beta} J_1 \mathbf{S}_i \cdot \mathbf{S}_j + \sum_{\langle i,j \rangle, i \in \alpha, j \in \alpha} J_2 \mathbf{S}_i \cdot \mathbf{S}_j, \quad (1)$$

and

$$\mathcal{H}_{\text{Zeeman}} = -h \sum_j S_j^z. \quad (2)$$

Here, \mathbf{S}_i denotes the $S = 1/2$ spin operator at site i , where the sites are the vertices of the square-kagome lattice shown in Fig. 1. The spin operator satisfies $\mathbf{S}_i^2 = S(S + 1)$. The sum of \mathcal{H}_0 runs over all the nearest-neighbor pairs in the square-kagome lattice. Energies are measured in units of J_1 ; hereafter, we set $J_1 = 1$. The number of spin sites is denoted by N_s , where $N_s/6$ is an integer. We treat $N_s = 24, 30, 36$, and 42 in this study. We impose the periodic boundary conditions for clusters with site N_s ; the shapes of the clusters are shown in Fig. 1. Note here that the shapes for $N_s = 24$ and 30 are squares although the latter is slightly tilted. On the other hand, the shapes for $N_s = 36$ and 42 are not squares. However, examination of systems with a large N_s would give a higher resolution of the magnetization process and contribute much to our understanding of this system. Note here that the same model including the

control of J_2 was previously examined in Refs. 46 and 47. Reference 46 treated this model within an effective Hamiltonian based on the localized-magnon picture. Reference 47 treated only $N_s = 24$ and 30. Both of these studies did not examine the magnetization jump at one-third of the height of the saturation on which we focus our attention in this study.

We calculate the lowest energy of \mathcal{H}_0 in the subspace belonging to $\sum_j S_j^z = M$ by numerical diagonalizations based on the Lanczos algorithm and/or Householder algorithm. The energy is denoted by $E(N_s, M)$, where M takes an integer value down from $M_{\text{low}} (=0)$ up to the saturation value $M_s (=SN_s)$. We use the normalized magnetization $m = M/M_s$. Some of the Lanczos diagonalizations were carried out using the MPI-parallelized code, which was originally developed in the study of Haldane gaps.⁴⁸ The usefulness of our program was previously confirmed in large-scale parallelized calculations.^{12,36,49} Note here that the calculations in cases of a small M for $N_s = 42$ require the use of the K computer (Kobe, Japan) to obtain the magnetization process of the entire range.

The magnetization process for a finite-size system is obtained by considering the magnetization increase from M to $M + 1$ in the field,

$$H = E(N_s, M + 1) - E(N_s, M), \quad (3)$$

under the condition that the lowest-energy state with the magnetization M and that with the magnetization $M + 1$ become the ground state in specific magnetic fields. It is often the case that the lowest-energy state with the magnetization M does not become the ground state in any field. In this case, the magnetization process around the magnetization M is determined by the Maxwell construction.^{4,5}

We evaluate the average local magnetization defined as

$$m_{\text{LM}}^\xi = \frac{1}{N_\xi} \sum_{j \in \xi} \langle S_j^z \rangle, \quad (4)$$

where ξ takes α and β . N_ξ denotes the number of ξ sites; namely, $N_\alpha = 2N_s/3$ and $N_\beta = N_s/3$. Here, the symbol $\langle \mathcal{O} \rangle$ represents the expectation value of the operator \mathcal{O} with respect to the lowest-energy state within the subspace characterized by a fixed magnetization M that we focus our attention on. Averaging over ξ is carried out when the ground-state level is degenerate. Note that, when the ground state belonging to M is not degenerate, the results do not change regardless of the presence or absence of this average. We also measure the correlation functions $\langle S_j^z S_k^z \rangle$ and $\langle S_j^x S_k^x \rangle$ to capture well the features of the wave functions that are numerically obtained.

3. Results and Discussion

First, we present our results of the J_2 dependence of the local magnetization of the $m = 1/3$ state, which are shown in Fig. 2. A similar examination concerning the parameter dependence was carried out in cases of the Cairo-pentagon lattice¹³ and the distorted kagome lattice,¹⁵ and the Lieb lattice accompanied by frustrating interaction.⁵⁰ One finds in Fig. 2(a) a large decrease in

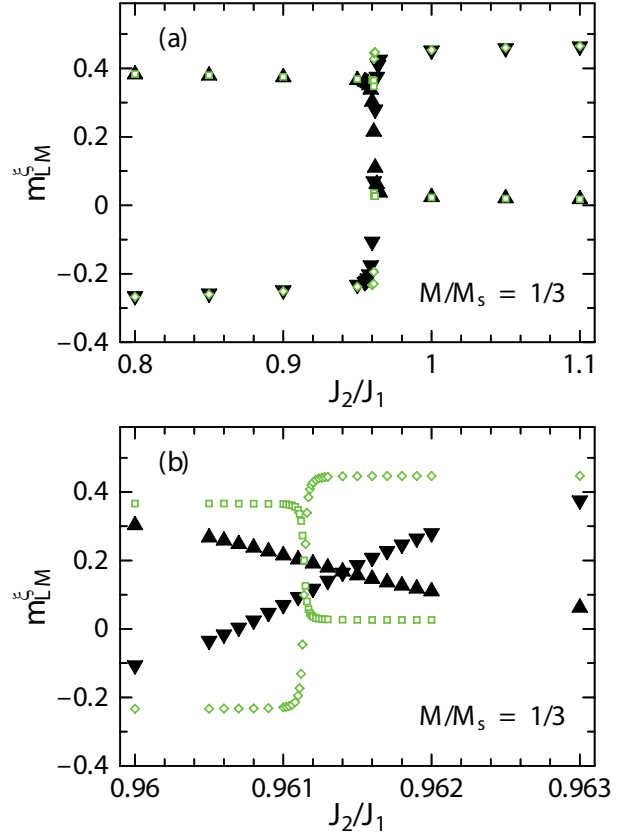


Fig. 2. (Color) Dependence of the local magnetization at $m = 1/3$ on the ratio of J_2/J_1 . Panel (b) is a zoom-in view of panel (a) to observe the range near the critical point in detail. Black closed triangles and inverted triangles denote $N_s = 24$ data of α and β , respectively. Green open squares and diamonds denote $N_s = 30$ data of α and β , respectively.

m_{LM}^α and a large increase in m_{LM}^β near $J_2/J_1 \sim 0.96$. This marked change suggests that a phase transition occurs between the ferrimagnetic state for $J_2/J_1 \lesssim 0.96$ and the state composed of singlet spins and almost fully polarized spins for $J_2/J_1 \gtrsim 0.96$. The phase transition has already been reported in Ref. 47, which concluded that this is a first-order transition. To detect the behavior of m_{LM}^ξ near $J_2/J_1 \sim 0.96$, we observe a detailed change in the zoom-in view in Fig. 2(b). Our results show a continuous change in m_{LM}^ξ for both $N_s = 24$ and 30 although the change for $N_s = 30$ is much more rapid than that for $N_s = 24$. From the observation of this continuous behavior, the conclusion of the first-order transition may be premature. Note also that the continuous change for $N_s = 30$ is in contrast to the discontinuous change for the same N_s in the case of the Cairo-pentagon lattice¹³ despite the fact that the present model and the model on the Cairo-pentagon lattice share the same number of spin sites in each unit cell. It is difficult within studies based on finite-size examinations, but it should be resolved in future studies to determine whether the transition is of the second or first order. An important point clarified in this study is that $J_2/J_1 = 1$ is different from the transition point ~ 0.96 and that $J_2/J_1 = 1$ is in the state composed of singlet spins in the α sites and almost fully polarized spins in the β sites. Hereafter, in the present

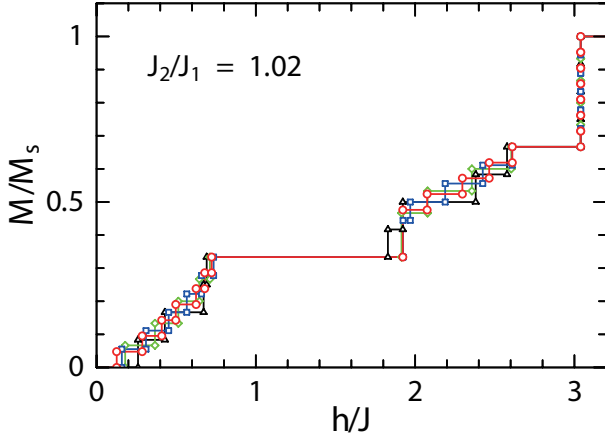


Fig. 3. (Color) Magnetization process for $J_2/J_1 = 1.02$. Black triangles, green diamonds, blue squares, and red circles denotes data for $N_s = 24, 30, 36,$ and 42 , respectively.

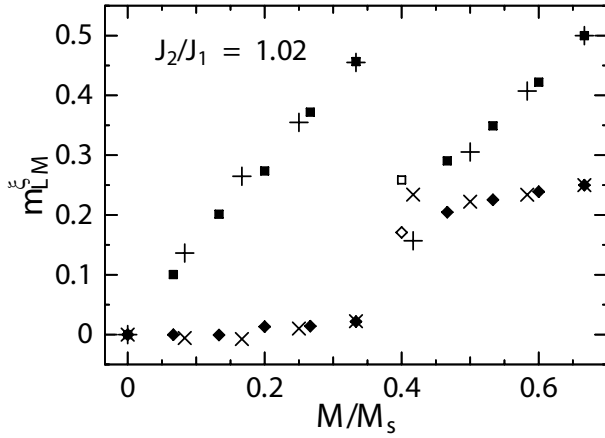


Fig. 4. Average local magnetization at $m = 1.02$. Pluses and crosses denote $N_s = 24$ data for α and β , respectively. Diamonds and squares denote $N_s = 30$ data for α and β , respectively. All the states are realized for $N_s = 24$, but not for $N_s = 30$. For $N_s = 30$, closed symbols represent data for the stably realized states, while open symbols denote data for the unstable states during the magnetization jump.

study, we focus on the case of the side of J_2/J_1 that is greater than the transition point $J_2/J_1 \sim 0.96$.

Next, we examine the magnetization process in the phase of the $J_2/J_1 = 1$ side. Our results are shown in Fig. 3 for $J_2/J_1 = 1.02$. This parameter is chosen within the same side as $J_2/J_1 = 1$ as a value close to $J_2/J_1 = 1$. Some features are shared between $J_2/J_1 = 1$ and 1.02 ; a detailed comparison between the results of $J_2/J_1 = 1$ and 1.02 will be carried out later. The magnetization processes in Fig. 3 show a clear existence of the $m = 1/3$ plateau. No jump appears for $N_s = 24$ at the edge of the higher-field side of the $m = 1/3$ height. For $N_s \geq 30$, on the other hand, magnetization jumps are clearly observed. The appearance of such jumps is independent of N_s , at least within $N_s \geq 30$ of the present finite-size-system study. In Fig. 4, the average local magnetizations for the square-cluster systems are shown. One easily finds that discontinuous behaviors

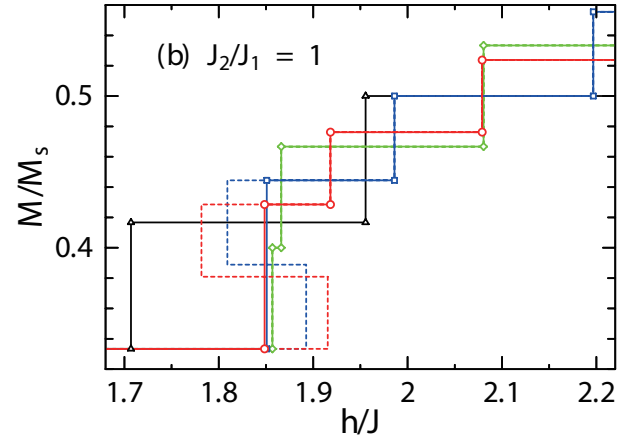
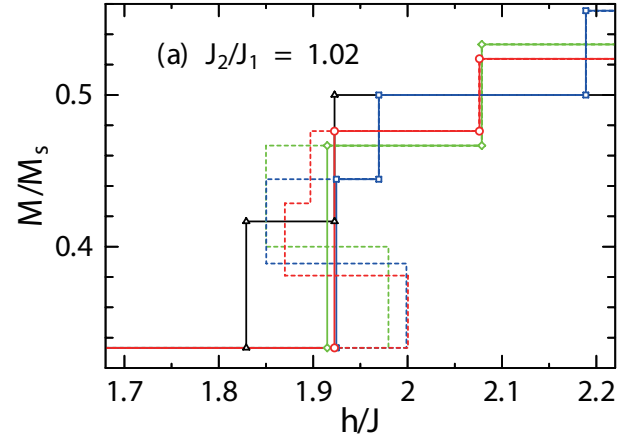


Fig. 5. (Color) Zoom-in views of the magnetization processes for (a) $J_2/J_1 = 1.02$ and (b) $J_2/J_1 = 1$. Symbols are the same as those in Fig. 3. The broken lines represent the results before the Maxwell construction is carried out.

in α and β sites appear between $M = (1/3)M_s$ and $M > (1/3)M_s$. At $M = (1/3)M_s$, our results suggest that a spin at a β site reveals almost a full moment along the z -axis and that spins at α sites form a singlet state in the small square inside each *shuriken*.

Let us next compare between the results of the magnetization processes for $J_2/J_1 = 1$ and 1.02 . Figures 5(a) and 5(b) show zoom-in views of the magnetization processes around the edge of the higher-field side of the $m = 1/3$ height. The most marked difference between the two cases is the skip δM in the results for $N_s = 42$; we observe $\delta M = 2$ for $J_2/J_1 = 1$ whereas we observe $\delta M = 3$ for $J_2/J_1 = 1.02$. The result of $\delta M = 3$ for $J_2/J_1 = 1.02$ is important from the viewpoint of the origin of the jump. A finite-size jump with $\delta M = 2$ can appear in the nematic phase,^{16,17} where the two-magnon bound state is realized. The nematic phase is gapless so that the magnetization process in the thermodynamic limit is continuous. Thus, the finite-size jump owing to the nematic phase is only a finite-size effect and does not become a macroscopic jump in the thermodynamic limit. The present result of $\delta M = 3$ for $N_s = 42$ and $J_2/J_1 = 1.02$ clearly excludes the possibility for the appearance of the finite-size jump owing to the nematic phase. The skip $\delta M = 3$ also suggests that the jump becomes a macroscopic one in

the thermodynamic limit.

Let us then estimate the skip in the thermodynamic limit from our finite-size results. The resolution of the normalized magnetization process is given by $2/N_s$. If a finite-size system reveals a jump with $\delta M = 2$, the skip δm of the normalized magnetization jump in the thermodynamic limit should satisfy

$$2/N_s < \delta m < 2(2/N_s), \quad (5)$$

while the skip is given by

$$\delta m > 2(2/N_s), \quad (6)$$

if a finite-size system reveals a jump with $\delta M = 3$. For $J_2/J_1 = 1.02$, we have $\delta M = 2$ for $N_s = 36$ and $\delta M = 3$ for $N_s = 42$; Eqs. (5) and (6) suggest

$$0.095 \lesssim \delta m \lesssim 0.111. \quad (7)$$

For $J_2/J_1 = 1$, on the other hand, we have $\delta M = 2$ for $N_s = 36$ and 42 and no jumps for $N_s \leq 30$, which suggest

$$\delta m \lesssim 0.095. \quad (8)$$

Therefore, one finds that the skip of the jump becomes larger when J_2/J_1 deviates from the critical point ~ 0.96 clarified in Fig. 2.

Table I. Correlation functions for $N_s = 24$ cluster at $J_2/J_1 = 1.02$. We select a pair of sites i and j so that the distance between these sites is largest in this cluster.

		$M = \frac{1}{3}M_s$	$M = \frac{1}{3}M_s + 1$	$M = \frac{1}{3}M_s + 2$
$i, j \in \alpha$	$\langle S_i^z S_j^z \rangle$	0.0005068	0.0571670	0.0498709
	$\langle S_i^x S_j^x \rangle$	0.0000012	0.0048659	0.0043312
$i, j \in \beta$	$\langle S_i^z S_j^z \rangle$	0.2071796	0.0335379	0.0960927
	$\langle S_i^x S_j^x \rangle$	0.0000184	0.0192386	0.0167820

Next, let us consider the spin direction from the data of correlation functions. We measure $\langle S_i^z S_j^z \rangle$ and $\langle S_i^x S_j^x \rangle$ between the pair of sites i and j , where i and j in the same group are the most distant in a finite-size cluster forming a square. The same analysis was carried out in Ref. 15. Within this study, the $N_s = 24$ cluster is the case that should be measured while the others are not because the $N_s = 42$ and 36 clusters do not form a square and because i and j as the most distant sites for the $N_s = 30$ cluster are not in the same group. Our present results are summarized for $J_2/J_1 = 1.02$ in Table I. Note here that, for $N_s = 24$, $M = (1/3)M_s$, $M = (1/3)M_s + 1$, and $M = (1/3)M_s + 2$ correspond to $m = 1/3$, $m = 0.4167$, and $m = 0.5$, respectively. From Eq. (7), it is clear that $m = 0.5$ is outside the jump, although it is unclear whether $m = 0.4167$ is outside or inside the jump because $m = 0.4167$ is very close to the upper edge of the jump. Therefore, it is reasonable to consider that the $M = (1/3)M_s + 2$ state is appropriate for observing a state under a field higher than the jump; on the other hand, the $M = (1/3)M_s$ state is appropriate for observing a state under a field lower than the jump. At $M = (1/3)M_s$, only $\langle S_i^z S_j^z \rangle$ for $i, j \in \beta$ is dominant; the other quantities are very small. These results are in agreement with the

behavior that we have observed in the m_{LM}^ξ . Thus, it is confirmed that, at $m = 1/3$, the system forms the state in which the spins at β sites have almost a full moment along the z -axis and where spins at α sites form a singlet state in the small square inside each *shuriken*. At $M = (1/3)M_s + 2$, on the other hand, the spin state is markedly different. $\langle S_i^z S_j^z \rangle$ for $i, j \in \beta$ is markedly smaller than that at $M = (1/3)M_s$ while $\langle S_i^z S_j^z \rangle$ for $i, j \in \alpha$ is larger. In addition, both $\langle S_i^x S_j^x \rangle$ for $i, j \in \alpha$ and $\langle S_i^x S_j^x \rangle$ for $i, j \in \beta$ are significantly nonzero. The results concerning the transverse component strongly suggest that α and β spins take directions that have nonzero angles from the z -axis. This picture concerning the state of $M = (1/3)M_s + 2$ is consistent with the speculation for $J_2/J_1 = 1$ presented in Ref. 6 as the umbrella-type spin state. Finally, note that the behavior at $M = (1/3)M_s + 1$ is qualitatively the same as that at $M = (1/3)M_s + 2$, although it is unclear whether the $m = 0.4167$ state is stable or unstable.

4. Conclusion and Remarks

In this paper, we study the spin-1/2 Heisenberg antiferromagnet on a square-kagome lattice with distortion by numerical-diagonalization calculations. We have found that the magnetization jump occurs at the higher-field edge of one-third of the height of the saturation as a frustration effect. An essential improvement from the results in Ref. 6 is that our large-scale calculations detect the behavior of the growth of the jump when the interactions in the small square in a *shuriken* become larger. Our finite-size results have clarified that a possibility of a finite-size jump owing to the spin-nematic state is excluded. Our analysis of spin-spin correlation functions is another essential improvement suggesting that, in the higher-field region, each spin reveals its own significant transverse component, while no transverse components are observed in the state at one-third of the height of the saturation. The changes in spin directions in the spin-isotropic system share the behavior in the spin-flop phenomenon observed in spin-anisotropic systems. Magnetization jumps in spin-isotropic systems were reported in several studies.^{51–59} The comparison between these cases and the present case will also be useful for understanding well the occurrence of these jumps. The present consequence of the magnetization jump will become a clue for future investigations, which would contribute much to our understanding of frustration effects in magnetic materials.

Acknowledgments

This work was partly supported by JSPS KAKENHI Grant Numbers 23340109 and 24540348. Nonhybrid thread-parallel calculations in numerical diagonalizations were based on TITPACK version 2 coded by H. Nishimori. This research used computational resources of the K computer provided by the RIKEN Advanced Institute for Computational Science through the HPCI System Research projects (Project ID: hp150024). Some of the computations were performed using facilities of the Department of Simulation Science, National

Institute for Fusion Science; Center for Computational Materials Science, Institute for Materials Research, Tohoku University; Supercomputer Center, Institute for Solid State Physics, The University of Tokyo; and Supercomputing Division, Information Technology Center, The University of Tokyo. This work was partly supported by the Strategic Programs for Innovative Research; the Ministry of Education, Culture, Sports, Science and Technology of Japan; and the Computational Materials Science Initiative, Japan. We would like to express our sincere thanks to the staff of the Center for Computational Materials Science of the Institute for Materials Research, Tohoku University, for their continuous support of the SR16000 supercomputing facilities.

- 1) Y. Narumi, M. Hagiwara, R. Sato, K. Kindo, H. Nakano, and M. Takahashi, *Physica B* **246**, 509 (1998).
- 2) H. Kageyama, Y. Ueda, Y. Narumi, K. Kindo, M. Kobayashi, M. Sato, and Y. Uwatoko, *Prog. Theor. Phys. Suppl.* **145** 17 (2002).
- 3) L. Néel, *Ann. Phys. Paris* **5**, 232 (1936).
- 4) M. Kohno and M. Takahashi, *Phys. Rev. B* **56**, 3212 (1997).
- 5) T. Sakai and M. Takahashi, *Phys. Rev. B* **60**, 7295 (1999).
- 6) H. Nakano and T. Sakai, *J. Phys. Soc. Jpn.* **82**, 083709 (2013).
- 7) R. Siddharthan and A. Georges: *Phys. Rev. B* **65**, 014417 (2001).
- 8) P. Tomczak and J. Richter, *J. Phys. A: Math. Gen.* **36**, 5399 (2003).
- 9) J. Richter, J. Schulenburg, P. Tomczak, and D. Schmalfß, *Condens. Matter Phys.* **12**, 507 (2009).
- 10) H. Nakano and T. Sakai, *J. Phys. Soc. Jpn.* **79**, 053707 (2010).
- 11) T. Sakai and H. Nakano, *Phys. Rev. B* **83**, 100405(R) (2011).
- 12) H. Nakano and T. Sakai, *J. Phys. Soc. Jpn.* **83**, 104710 (2014).
- 13) H. Nakano, M. Isoda, and T. Sakai, *J. Phys. Soc. Jpn.* **83**, 053702 (2014).
- 14) M. Isoda, H. Nakano, and T. Sakai, *J. Phys. Soc. Jpn.* **83**, 084710 (2014).
- 15) H. Nakano, T. Sakai, and Y. Hasegawa, *J. Phys. Soc. Jpn.* **83**, 084709 (2014).
- 16) T. Momoi, P. Sindzingre, and K. Kubo, *Phys. Rev. Lett.* **108**, 057206 (2012).
- 17) N. Shannon, T. Momoi, and P. Sindzingre, *Phys. Rev. Lett.* **96**, 027213 (2006).
- 18) M. P. Shores, E. A. Nytko, B. M. Bartlett, and D. G. Nocera, *J. Am. Chem. Soc.* **127**, 13462 (2005).
- 19) P. Mendels and F. Bert, *J. Phys. Soc. Jpn.* **79**, 011001 (2010).
- 20) H. Yoshida, Y. Okamoto, T. Tayama, T. Sakakibara, M. Tokunaga, A. Matsuo, Y. Narumi, K. Kindo, M. Yoshida, M. Takigawa, and Z. Hiroi, *J. Phys. Soc. Jpn.* **78**, 043704 (2009).
- 21) M. Yoshida, M. Takigawa, H. Yoshida, Y. Okamoto, and Z. Hiroi, *Phys. Rev. Lett.* **103**, 077207 (2009).
- 22) H. Ishikawa, M. Yoshida, K. Nawa, M. Jeong, S. Krämer, M. Horvatić, C. Berthier, M. Takigawa, M. Akaki, A. Miyake, M. Tokunaga, K. Kindo, J. Yamaura, Y. Okamoto, and Z. Hiroi, *Phys. Rev. Lett.* **114**, 227202 (2015).
- 23) Y. Okamoto, H. Yoshida, and Z. Hiroi, *J. Phys. Soc. Jpn.* **78**, 033701 (2009).
- 24) Y. Okamoto, M. Tokunaga, H. Yoshida, A. Matsuo, K. Kindo, and Z. Hiroi, *Phys. Rev. B* **83**, 180407 (2011).
- 25) P. Lecheminant, B. Bernu, C. Lhuillier, L. Pierre, and P. Sindzingre, *Phys. Rev. B* **56**, 2521 (1997).
- 26) C. Waldtmann, H.-U. Everts, B. Bernu, C. Lhuillier, P. Sindzingre, P. Lecheminant, and L. Pierre, *Eur. Phys. J. B* **2**, 501 (1998).
- 27) K. Hida, *J. Phys. Soc. Jpn.* **70**, 3673 (2001).
- 28) D. C. Cabra, M. D. Grynberg, P. C. W. Holdsworth, and P. Pujol, *Phys. Rev. B* **65**, 094418 (2002).
- 29) J. Schulenburg, A. Honecker, J. Schnack, J. Richter, and H.-J. Schmidt, *Phys. Rev. Lett.* **88**, 167207 (2002).
- 30) A. Honecker, J. Schulenburg, and J. Richter, *J. Phys.: Condens. Matter* **16**, S749 (2004).
- 31) D. C. Cabra, M. D. Grynberg, P. C. W. Holdsworth, A. Honecker, P. Pujol, J. Richter, D. Schmalfß, and J. Schulenburg, *Phys. Rev. B* **71**, 144420 (2005).
- 32) O. Cépas, C. M. Fong, P. W. Leung, and C. Lhuillier, *Phys. Rev. B* **78**, 140405(R) (2008).
- 33) H. C. Jiang, Z. Y. Weng, and D. N. Sheng, *Phys. Rev. Lett.* **101**, 117203 (2008).
- 34) P. Sindzingre and C. Lhuillier, *Europhys. Lett.* **88**, 27009 (2009).
- 35) H. Nakano, T. Shimokawa, and T. Sakai, *J. Phys. Soc. Jpn.* **80**, 033709 (2011).
- 36) H. Nakano and T. Sakai, *J. Phys. Soc. Jpn.* **80**, 053704 (2011).
- 37) A. Honecker, D. C. Cabra, H.-U. Everts, P. Pujol, and F. Stauffer, *Phys. Rev. B* **84**, 224410 (2011).
- 38) S. Yan, D. A. Huse, and S. R. White, *Science* **332**, 1173 (2011).
- 39) S. Depenbrock, I. P. McCulloch, and U. Schollwöck, *Phys. Rev. Lett.* **109**, 067201 (2012).
- 40) S. Capponi, O. Derzhko, A. Honecker, A. M. Läuchli, and J. Richter, *Phys. Rev. B* **88**, 144416 (2013).
- 41) S. Nishimoto, N. Shibata, and C. Hotta, *Nat. Commun.* **4**, 2287 (2013).
- 42) T. Sakai and H. Nakano, *Phys. Status Solidi B* **250**, 579 (2013).
- 43) H. Nakano and T. Sakai, *JPS Conf. Proc.* **3**, 014003 (2014).
- 44) Y. Iqbal, D. Poilblanc, and F. Becca, *Phys. Rev. B* **89**, 020407(R) (2014).
- 45) Y. Iqbal, D. Poilblanc, and F. Becca, *Phys. Rev. B* **91**, 020402(R) (2015).
- 46) O. Derzhko, J. Richter, O. Krupnitska, and T. Krokhnalskii, *Phys. Rev. B* **88**, 094436 (2013).
- 47) I. Rousochatzakis, R. Moessner, and van den Brink, *Phys. Rev. B* **88**, 195109 (2013).
- 48) H. Nakano and A. Terai, *J. Phys. Soc. Jpn.* **78**, 014003 (2009).
- 49) H. Nakano, S. Todo, and T. Sakai, *J. Phys. Soc. Jpn.* **82**, 043715 (2013).
- 50) H. Nakano and T. Sakai, *Jpn. J. Appl. Phys.* **54**, 030305 (2015).
- 51) K. Kubo and T. Momoi, *Z. Phys.* **103**, 485 (1997).
- 52) T. Momoi, H. Sakamoto, and K. Kubo, *Phys. Rev. B* **59**, 9491 (1999).
- 53) A. Honecker, F. Mila, and M. Troyer, *Eur. Phys. J. B* **15**, 227 (2000).
- 54) T. Momoi and K. Totsuka, *Phys. Rev. B* **62**, 15067 (2000).
- 55) K. Penc, N. Shannon, and H. Shiba, *Phys. Rev. Lett.* **93**, 197203 (2004).
- 56) C. Schröder, H. J. Schmidt, J. Schnack, and M. Luban, *Phys. Rev. Lett.* **94**, 207203 (2005).
- 57) N. P. Konstantinidis, *Phys. Rev. B* **72**, 064453 (2005).
- 58) J.-B. Fouet, F. Mila, D. Clarke, H. York, O. Tchernyshyov, P. Fendley, and R. M. Noack, *Phys. Rev. B* **73**, 214405 (2006).
- 59) F. Michaud, T. Coletta, S. R. Manmana, J.-D. Picon, and F. Mila, *Phys. Rev. B* **81**, 014407 (2010).